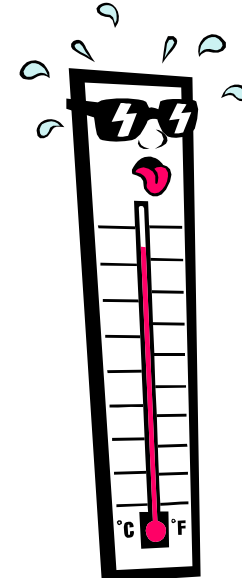


Calorimetry & Jet Finding

- Calorimetry:
 - Interactions of charged particles and photons
 - Electromagnetic cascades
 - Nuclear interactions
 - Hadronic cascades
- Calorimeters
 - Homogeneous calorimeters
 - Sampling calorimeters
- Jet Finding
 - Kinematics
 - Event shapes
 - Jet finding algorithms



Basic Principle

□ Calorimetry:

- measure energy by absorbing radiation
- analogous to temperature measurement for heat absorption

□ Detector:

- use massive detector to stop the particles → measure response
- response proportional to energy
- works for charged (e^\pm and hadrons) and neutral particles (neutrons, photons)
- segmentation → spatial resolution

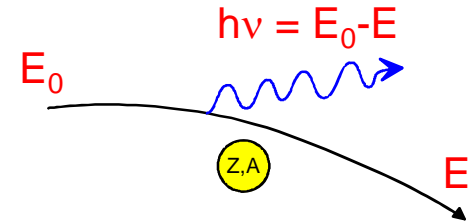
□ How does calorimetry work?

- formation of electromagnetic and/or hadronic showers
- energy converted into ionisation or excitation of matter → visible energy fraction
- detection by many different mechanisms:
 - scintillation
 - Cherenkov light
 - ionisation
 - dE/dx
- 2 modes: homogeneous or sampling

Recap: Bremsstrahlung

- Photon emission in nucleon field:

$$-\frac{dE}{dx} = 4\alpha N_A \frac{Z^2}{A} z^2 \left(\frac{1}{4\pi\epsilon_0} \frac{e^2}{mc^2} \right)^2 E_0 \ln \frac{183}{Z^{1/3}} \propto \frac{E_0}{m^2}$$



- Important only for e^+ and e^- : $\frac{\left(-\frac{dE}{dx} \Big|_{Brems} (e^\pm) \right)}{\left(-\frac{dE}{dx} \Big|_{Brems} (\mu^\pm) \right)} \approx 40000$

- Radiation length X_0 :

$$-\frac{dE}{E_0} = \frac{dx}{X_0} \quad \langle E \rangle = E_0 e^{-x/X_0}$$

- Critical energy $E_c(e)$:

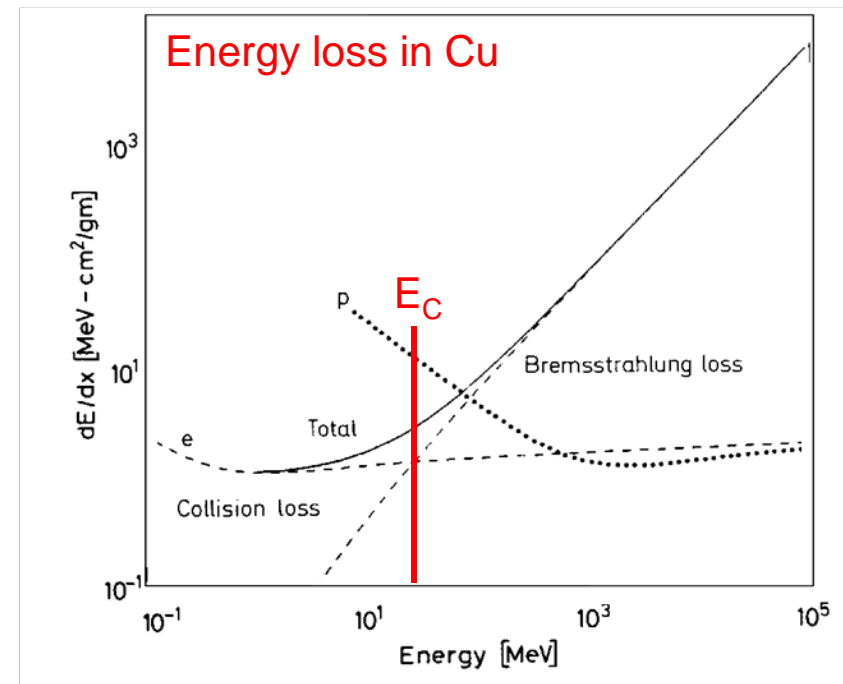
$$\frac{dE}{dx}(E_c) \Big|_{Brems} = \frac{dE}{dx}(E_c) \Big|_{ion}$$

- due to density effect in the relativistic rise:

$$E_c^{solid+liq} = \frac{610 \text{ MeV}}{Z + 1.24} \quad E_c^{gas} = \frac{710 \text{ MeV}}{Z + 1.24}$$

- For Fe ($Z=26$):

- $E_c(e) = 24 \text{ MeV}$
- $E_c(\mu) = 1 \text{ TeV}$



Recap: Pair Production

□ For momentum conservation:

- Coulomb field of nucleus (electron) needed to absorb recoil
- minimum energy: $E_\gamma \geq 2m_e c^2$

□ Related to Bremsstrahlung by substitution

□ Cross-section:

- low energy limit: $2 \ll \varepsilon \ll 137/Z^{1/3}$

$$\sigma_{pair} \approx 4\alpha r_e^2 Z^2 \left(\frac{7}{9} \ln 2\varepsilon \right)$$

- high energy limit: $\varepsilon \gg 137/Z^{1/3}$

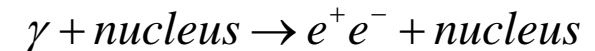
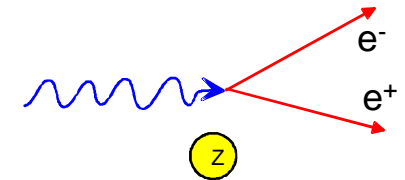
$$\sigma_{pair} \approx 4\alpha r_e^2 Z^2 \left(\frac{7}{9} \ln \frac{183}{Z^{1/3}} \right) \approx \frac{7}{9} \frac{A}{N_A} \frac{1}{X_0} \approx \frac{A}{N_A} \frac{1}{\lambda_{pair}}$$

Independent of energy

□ Mean free path: λ_{pair}

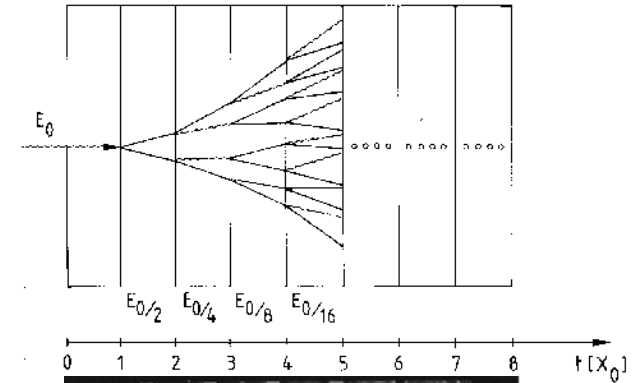
- Radiation length X_0

$$\lambda_{pair} = \frac{9}{7} X_0 \quad \left[\frac{g}{cm^2} \right]$$



Electromagnetic Cascades - Evolution

- High energy electron or photon starts shower:
 - Bremsstrahlung (γ emission) and pair production alternate
 - statistical process
 - in average: equal split of energy between particles
 - until energy drops below critical energy E_C where loss due to collision halt the cascade

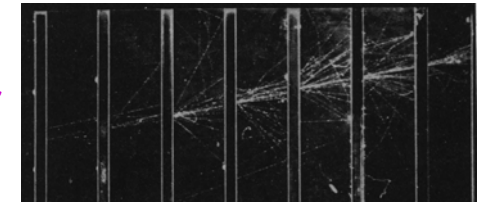


- Simple model: after t radiation lengths:

- number of particles (e^- , e^+ , γ): $N \cong 2^t$
- average energy:

$$E(t) \cong \frac{E_0}{2^t}$$

Electron shower in cloud chamber with Pb absorber



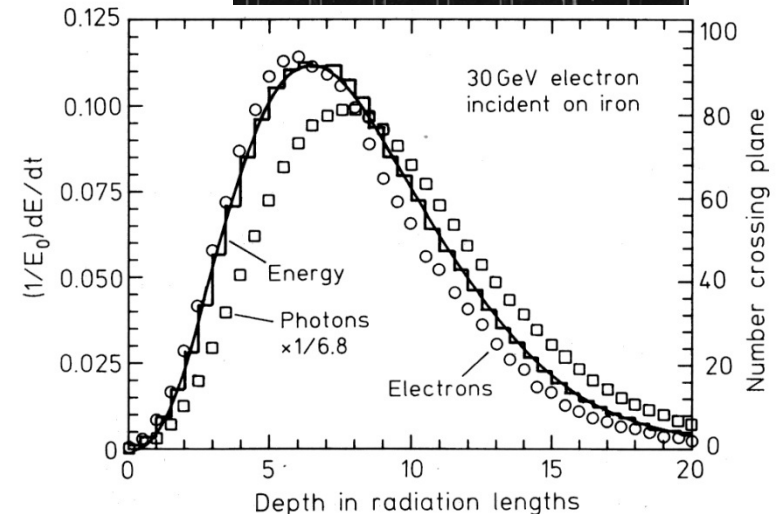
- Maximum penetration depth:

- assume abrupt stop at E_C :

$$E(t_{\max}) \cong \frac{E_0}{2^{t_{\max}}} = E_C$$

$$t_{\max} = \frac{1}{\ln 2} \ln \frac{E_0}{E_C}$$

- maximum number of particles: $N_{\max} \cong \frac{E_0}{E_C}$



Elmag. Cascades – Shower Profile

□ Longitudinal shower profile / energy deposit:

- slower than exponential rise
- shower maximum
- exponential decay

$$t_{\max} = \ln \frac{E_0}{E_c} \frac{1}{\ln 2}$$

□ Shower containment:

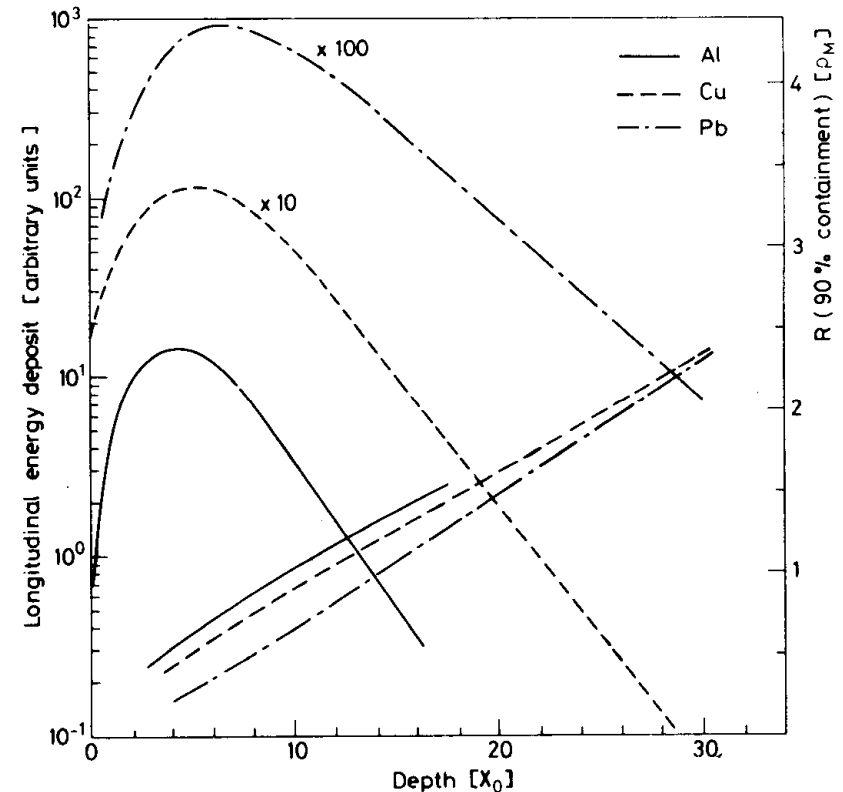
- reasonable to measure: 95% containment

$$t_{95\%} \approx t_{\max} + 0.08Z + 9.6$$

- e.g. 100 GeV shower in BGO:

$$E_c = 10.5 \text{ MeV}, \quad t_{\max} = 13 X_0, \quad t_{95\%} = 23 X_0$$

- size grows logarithmically with E_0
- size scales with X_0



(C. Fabjan, T. Ludlam, CERN-EP/82-37)

□ Transverse shower profile:

- Moliere radius:
- 95% E_0 within $2 R_M$
- 99% E_0 within $4 R_M$

$$R_M = \frac{21 \text{ MeV}}{E_c} X_0 \left[\frac{g}{\text{cm}^2} \right]$$

Elmag. Cascades – Energy Resolution

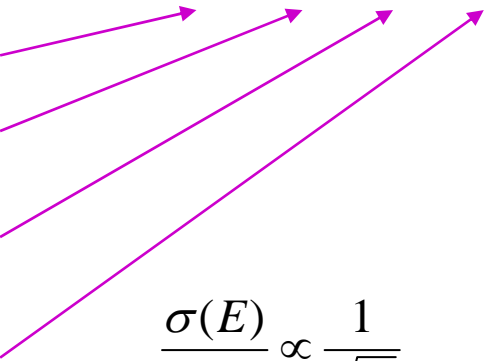
Fluctuations:

- due stochastic processes
- e.g. # of photons produced in scintillator: n
- Poisson \rightarrow Gaussian for large $\langle n \rangle$
- \rightarrow resolution improves with energy
- sampling: less signal \rightarrow larger fluctuation
- sampling: larger $Z \rightarrow$ larger angle \rightarrow smaller sampling fraction \rightarrow worse resolution...
- intrinsic limit: additional effects contribute

$$\frac{\sigma(E)}{E} \propto \frac{\sigma_s}{S} \propto \frac{\sqrt{n}}{n} \propto \frac{1}{\sqrt{n}} \propto \frac{1}{\sqrt{E}}$$

General energy resolution formula:

- stochastic term
- constant term
 - non-linearities, inhomogenities, calibration
- noise term
 - electronics resolution corresponds to fixed energy
- additional signal degradation: e.g. shower leakage
 - lateral leakage:
 - longitudinal leakage: fraction f

$$\frac{\sigma(E)}{E} = \frac{a}{\sqrt{E}} \oplus b \oplus \frac{c}{E} \oplus X$$


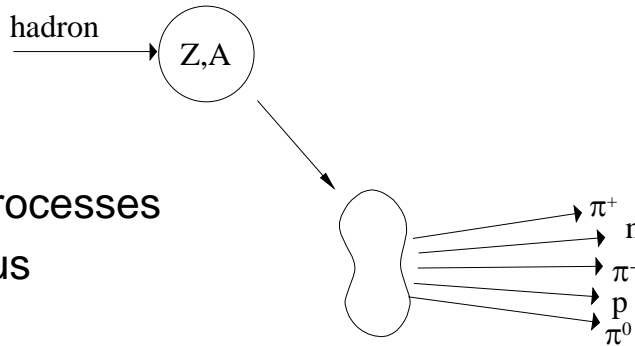
$$\frac{\sigma(E)}{E} \propto \frac{1}{\sqrt[4]{E}}$$

$$\frac{\sigma(E)}{E} \propto 1 + 4f + 50f^2$$

Nuclear Interactions

Charged particle interactions:

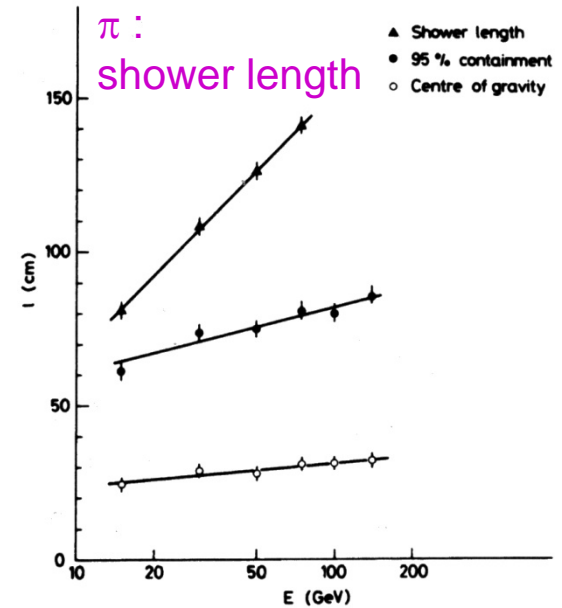
- for π , K, p; but not μ
- with $E > \sim 5\text{GeV}$
- dominated by inelastic nuclear processes
- excitation and break-up of nucleus
- produce secondary particles



Particle multiplicity of inelastic scattering: $\propto \ln(E)$

Cross sections:

- depends on A of calorimeter material
- but little on particle energies for $E > 1\text{ GeV}$



$$\sigma_{inel} \approx \sigma_0 A^{0.7} \quad \sigma_0 \approx 35\text{ mb}$$

Nuclear (hadronic) absorption length: λ , λ_a

- scale of spatial development of had. shower
- e.g. iron: $\lambda_a = 16.8\text{cm}$ \rightarrow typical shower size of 100GeV π^- : 2m long, 60cm wide

$$\lambda_a = \frac{A}{N_A \rho \sigma_{inel}} \propto A^{\frac{1}{4}} \quad \text{because } \sigma_{inel} \approx \sigma_0 A^{0.7}$$

Nuclear (hadronic) interaction (collision) length: λ_{had} , λ_T

- mean free path (like for photons)

$$\lambda_{had} = \frac{A}{N_A \rho \sigma_{total}} \propto A^{\frac{1}{3}} \quad \lambda_{had} < \lambda_a$$

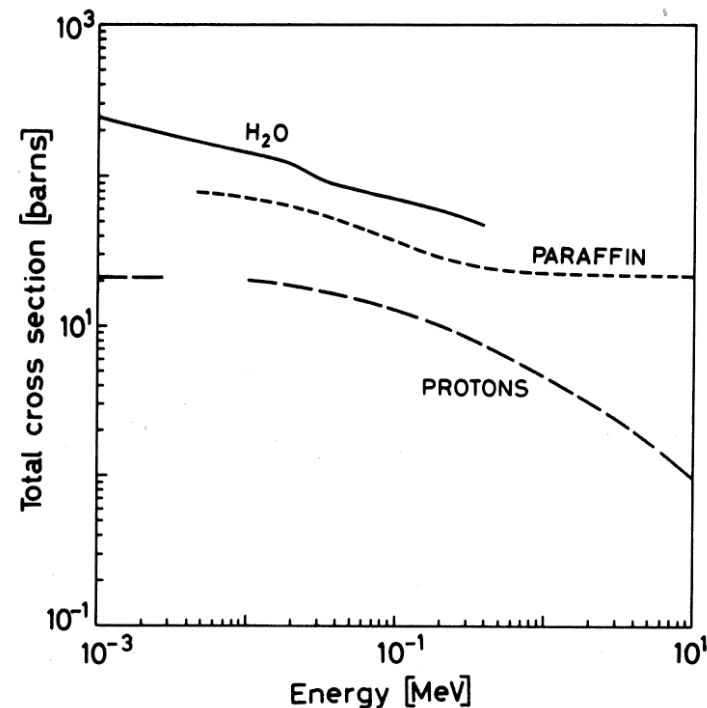
Neutrons

□ Neutron detection:

- only strong interaction: needs $\sim 10^{-15}\text{m}$ distance to nuclei
- \rightarrow much rarer process
- \rightarrow neutrons are very penetrating
- large scattering angles

□ Processes: $\sigma_{\text{tot}} = \sum \sigma_i$

- high energy hadron shower: $np \rightarrow X, nn \rightarrow X$
- elastic scattering off nuclei: $A(n,n)A$
- inelastic scattering: $A(n,n')A^* + \gamma, A(n,2n')B + \gamma$
- radiative neutron capture: $n + (Z,A) \rightarrow \gamma + (Z,A+1)$
- nuclear reactions: $(n,p), (n,d), (n,\alpha), \dots$
- fission: (n,f)



- $E_n > 100\text{MeV}$
- dominant for $E_n \text{ O}(\text{MeV})$
- $E_n > 1\text{MeV}$
- low v_n and resonances
- $E_n \text{ O}(\text{eV}) \dots \text{O}(\text{keV})$
- E_n thermal

Hadronic Cascades I

□ Hadronic component:

- charged hadrons: π , K, p
- neutral particles: soft γ , neutrons (need recoil p, i.e. H)
- low-E protons: 10-100 x ionisation of MIP

□ Invisible component:

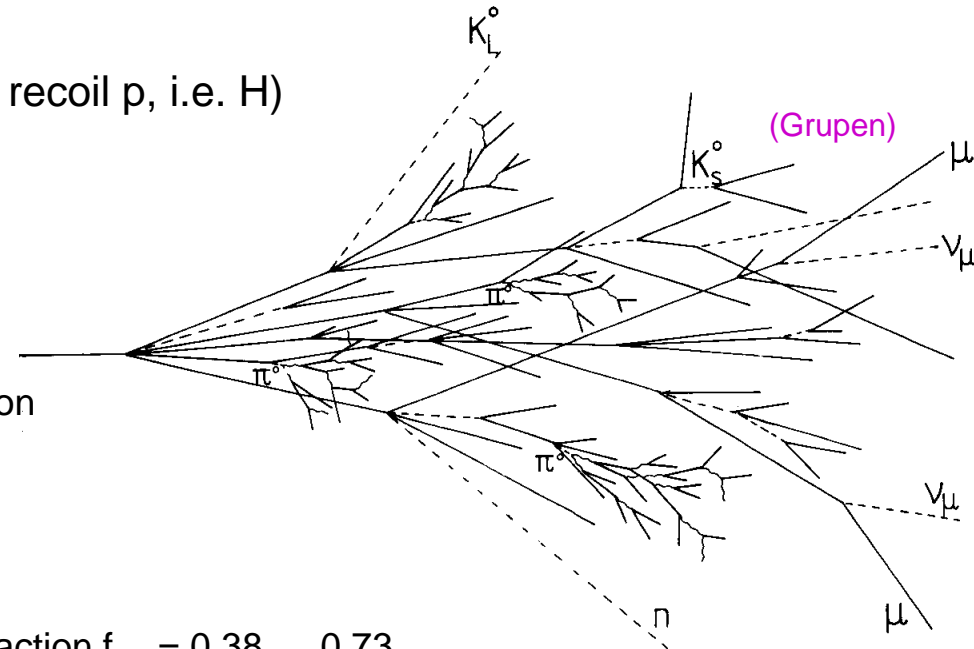
- ν and μ from π decay
- fission and spallation products:
 - low-E γ , π and neutrons \rightarrow secondary spallation
 - nuclear fragments \rightarrow stopped in absorber
 - low-E electromagnetic component:

□ Electromagnetic component:

- $\pi^0 \rightarrow \gamma\gamma$ initiate el.mag. cascade
 - ratio $\pi^0 / (\pi^+ + \pi^-)$ fluctuates
- fraction $f_{em} = 0.38 \dots 0.73$
for 10 ... 1000 GeV

□ Energy resolution:

- limited due to large fluctuations
- lower sampling fraction
- poorer shower containment



Hadronic Cascades II

□ Longitudinal shower profile:

$$t_{\max}(\lambda_T) \approx 0.2 \ln E[\text{GeV}] + 0.7$$

$$t_{95\%} \approx a \ln E + b$$

- e.g. iron: $a = 9.4\text{cm}$, $b = 39\text{cm}$

$$E = 100 \text{ GeV} \rightarrow t_{95\%} \approx 82 \text{ cm}$$

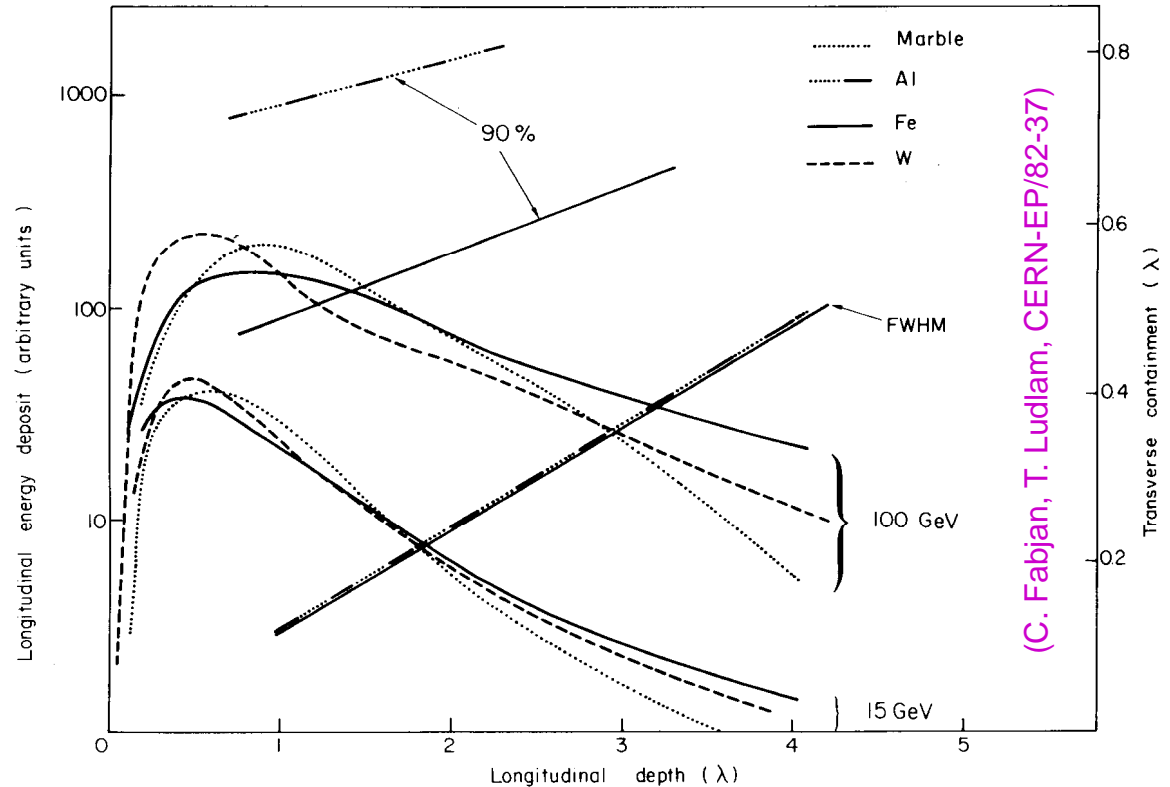
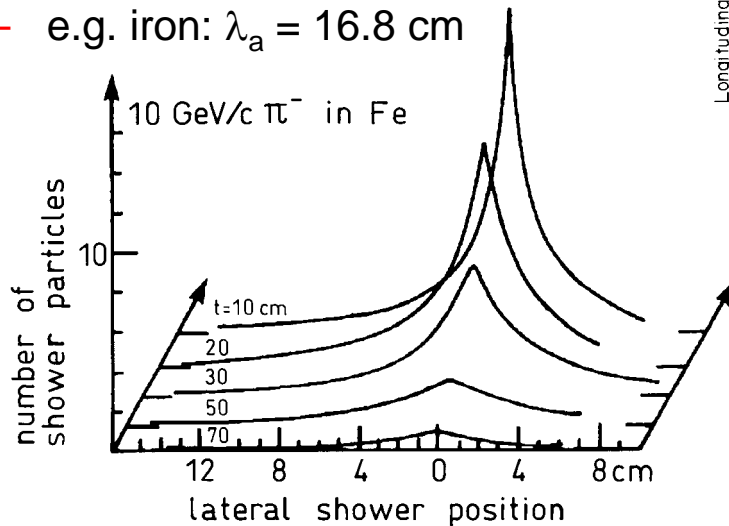
$$\rightarrow t_{100\%} \approx 200 \text{ cm}$$

□ Lateral shower profile:

- core & halo

- 95% containment

- e.g. iron: $\lambda_a = 16.8 \text{ cm}$



→ Hadronic showers:

- much longer

- and broader than electromagnetic showers

Interaction Lengths

Table 5. Radiation length X_0 , critical energy E_c and hadronic absorption length λ_{had} for some materials

Material	X_0 (g/cm ²)	E_c (MeV)	λ_{had} (g/cm ²)
H ₂	63	340	52.4
Al	24	47	106.4
Ar	18.9	35	119.7
Kr	11.3	21.5	147
Xe	8.5	14.5	168
Fe	13.8	24	131.9
Pb	6.3	6.9	193.7
Lead glass SF 5	9.6	~11.8	
Plexiglas	40.5	80	83.6
H ₂ O	36	93	84.9
NaI(Tl)	9.5	12.5	152.0
Bi ₄ Ge ₃ O ₁₂	8.0	10.5	164

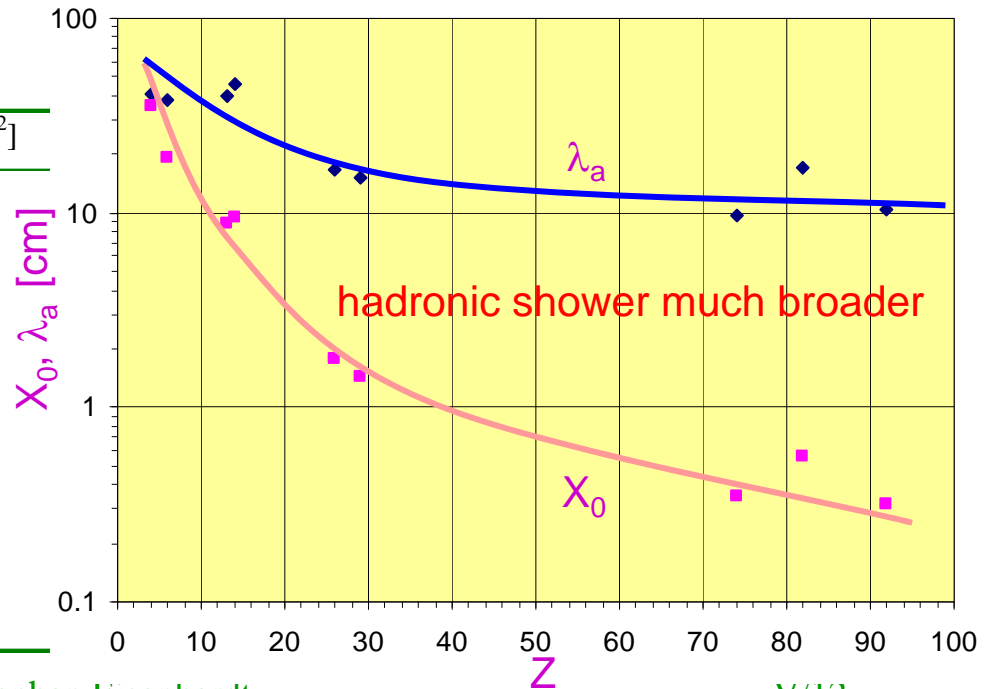
hadronic
shower
much
longer

- Radiation length X_0 :

$$-\frac{dE}{E_0} = \frac{dx}{X_0} \quad \langle E \rangle = E_0 e^{-x/X_0}$$

- Interaction length λ_T :

$$N(x) = N_0 e^{-\frac{x}{\lambda_{had}}}$$

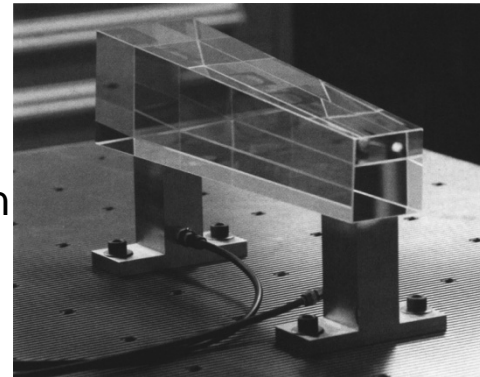


Material	Z	A	ρ [g/cm ³]	X_0 [g/cm ²]	λ_{had} [g/cm ²]
Hydrogen (gas)	1	1.01	0.0899 (g/l)	63	50.8
Helium (gas)	2	4.00	0.1786 (g/l)	94	65.1
Beryllium	4	9.01	1.848	65.19	75.2
Carbon	6	12.01	2.265	43	86.3
Nitrogen (gas)	7	14.01	1.25 (g/l)	38	87.8
Oxygen (gas)	8	16.00	1.428 (g/l)	34	91.0
Aluminium	13	26.98	2.7	24	106.4
Silicon	14	28.09	2.33	22	106.0
Iron	26	55.85	7.87	13.9	131.9
Copper	29	63.55	8.96	12.9	134.9
Tungsten	74	183.85	19.3	6.8	185.0
Lead	82	207.19	11.35	6.4	194.0
Uranium	92	238.03	18.95	6.0	199.0

Calorimeters

□ Homogeneous calorimeters:

- detector = absorber
- good energy resolution
- limited spatial resolution in longitudinal direction
- only for electromagnetic calorimeters



lead-glass medium
with pointing geometry

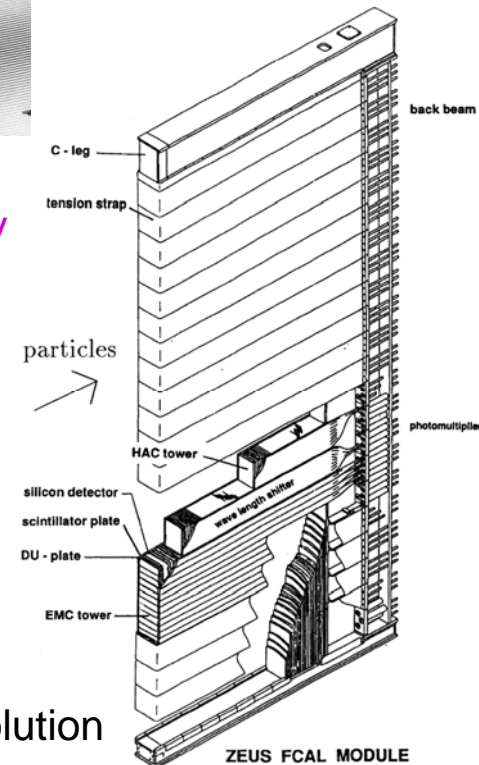
□ Sampling calorimeters:

- intersperse detectors and absorbers
- only fraction of energy is sampled
- limited energy resolution
- good spatial resolution
- for hadronic and electromagnetic calorimeters

□ Ideal calorimeter:

- coverage of full solid angle of experiment: no holes, highly segmented
- measurement of energy and position: good energy and spatial resolution
- fast response for trigger: dependent on cross section and luminosity
- within limitations of : technology, space, time, budget

ZEUS
FCAL module



Homogeneous Calorimeters I

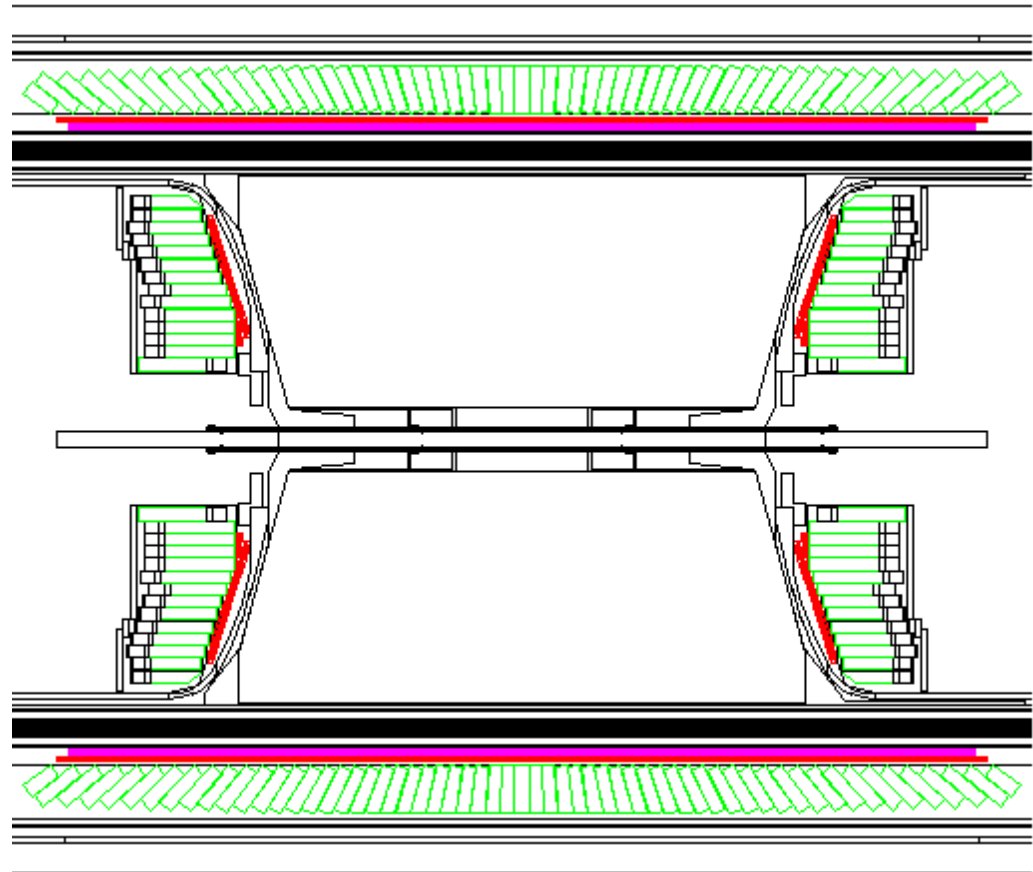
□ OPAL barrel & end-cap: lead/glass + presampler

- ≈ 10500 blocks: $10 \times 10 \times 37 \text{ cm}^3$, $24.6 X_0$
- spatial resolution (intrinsic) $\approx 11 \text{ mm}$ at 6 GeV
- readout:
 - barrel: photo multiplier
 - end-cap: photo triode

(OPAL collab. NIM A 305 (1991) 275)

- resolution:

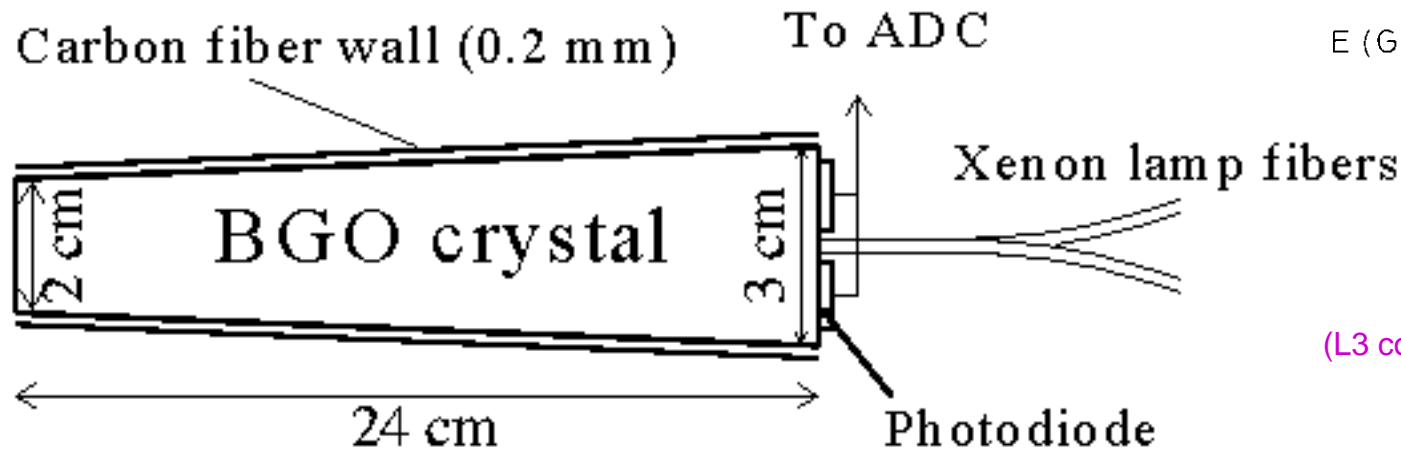
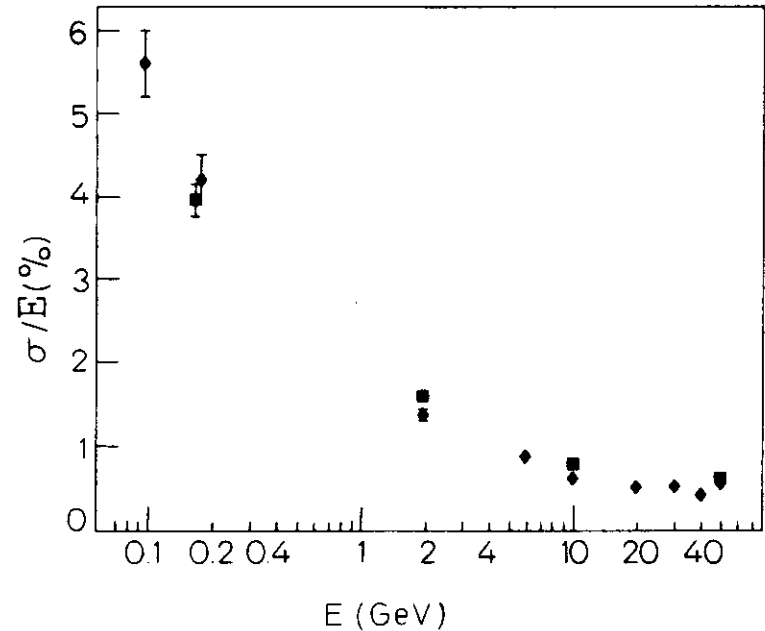
$$\frac{\sigma(E)}{E} = \frac{6\%}{\sqrt{E}} \oplus 0.2\%$$



Homogeneous Calorimeters II

□ L3 BGO el.mag. calorimeter:

- ≈ 11000 crystals, $21.4 X_0$
- cell size: $20 \times 20 \text{ mm}$
- spatial resolution $< 2 \text{ mm}$ ($E > 2 \text{ GeV}$)
- temperature monitoring + control system:
light output: $-1.55\% / ^\circ\text{C}$
- resolution:
 $\sigma_E/E < 1\%$ for $E > 5 \text{ GeV}$ (world record!)



(L3 collab. NIM A 289 (1991) 53)

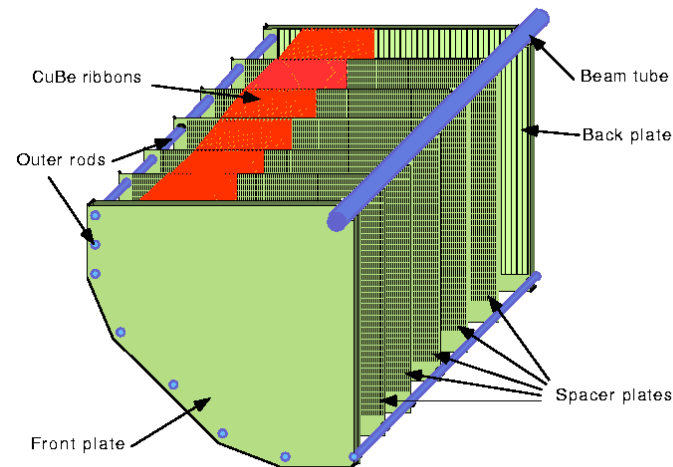
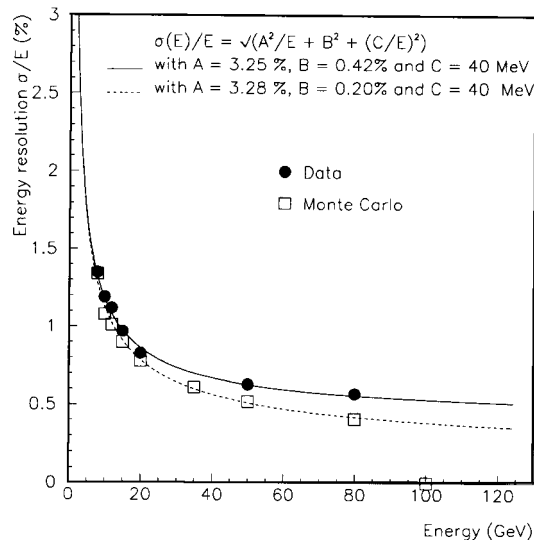
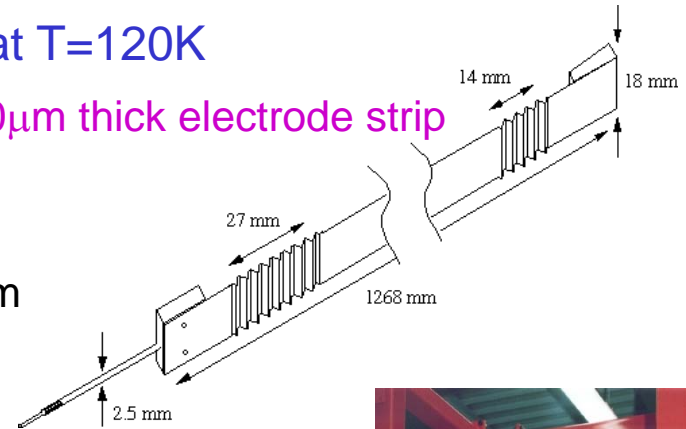
Homogeneous Calorimeters III

□ NA48 liquid Kr calorimeter: ionisation chamber at T=120K

- 13250 cells, 2x2x127cm³, 27 X₀
- spatial resolution: $\frac{4.2}{\sqrt{E}} + 0.6\text{mm}$
- time resolution: $\sigma_t \sim 0.25\text{ns}$
- needs control of impurities (O₂, N₂, H₂O) to <2ppm
- resolution:

$$\frac{\sigma(E)}{E} = \frac{3.2\%}{\sqrt{E}} \oplus \frac{10\%}{E} \oplus 0.5\%$$

40μm thick electrode strip

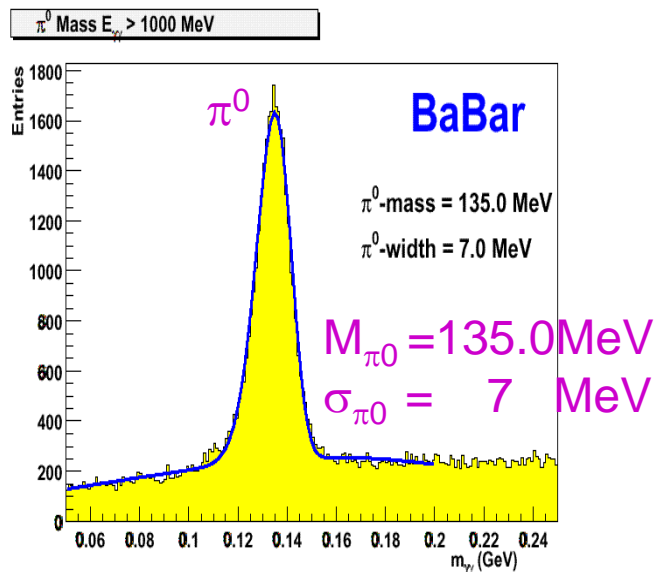
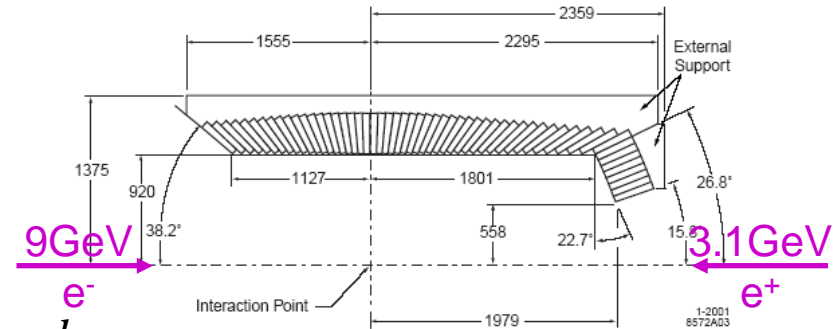


Homogeneous Calorimeters IV

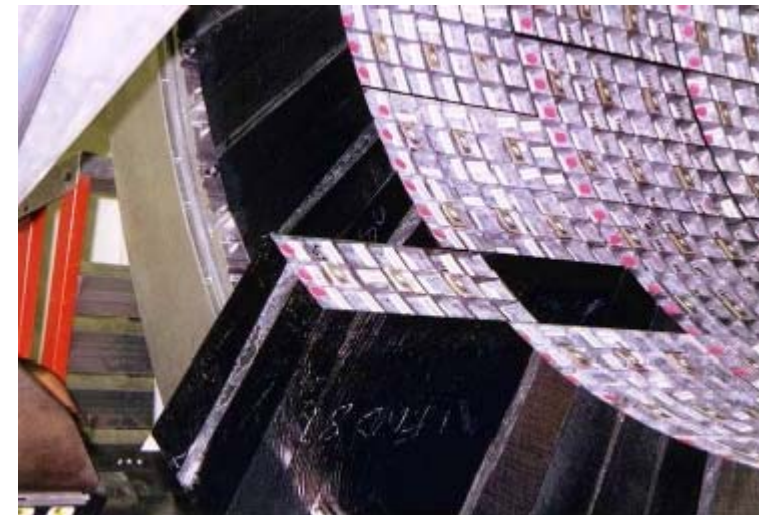
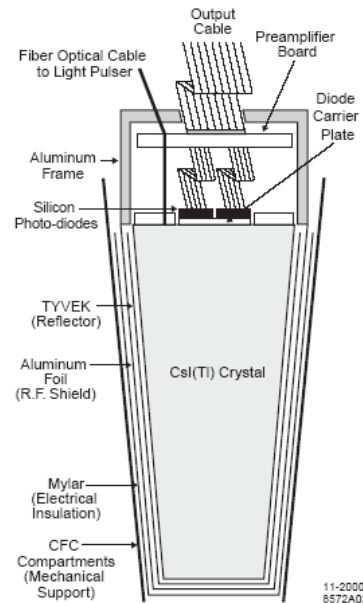
□ BaBar Csl el.mag. calorimeter:

- 6580 Csl(Tl) crystals, pointing geometry
- barrel: 48 azimuthal rings, forward: 8 rings
- PIN photodiode readout
- energy and angular resolution:

$$\frac{\sigma(E)}{E} = \frac{2.32\%}{\sqrt[4]{E}} \oplus 1.85\% \quad \sigma_{\theta,\phi}^{\text{design}} = \frac{3\text{mrad}}{\sqrt{E}} \oplus 2\text{mrad}$$



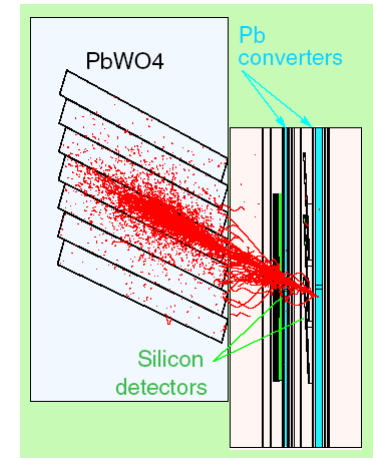
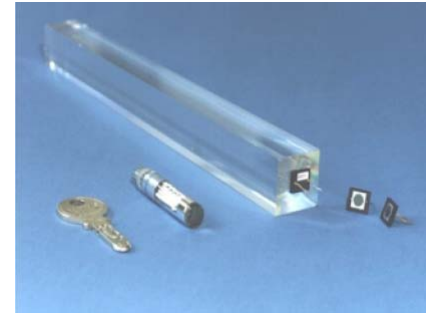
EMC performance



Homogeneous Calorimeters V

□ CMS lead-tungstate el.mag. calorimeter:

- 80000 PbWO_4 crystals (98%_{mass} metal)
- $26 X_0 = 23\text{cm}$, $22 \times 22\text{mm}^2$ front-face = R_M
- pointing geometry, inside 4T solenoid
- radiation dose: 1-2kGy/year → colours crystal
- avalanche photodiode readout
- stochastic energy resolution:

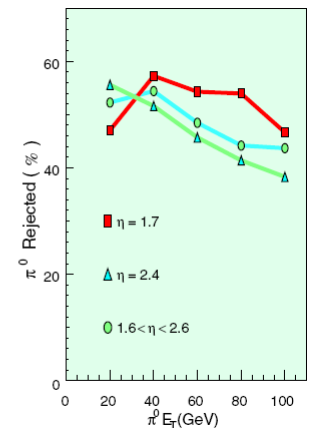
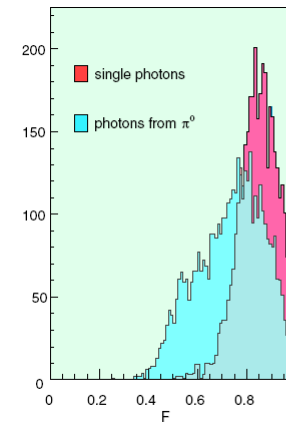
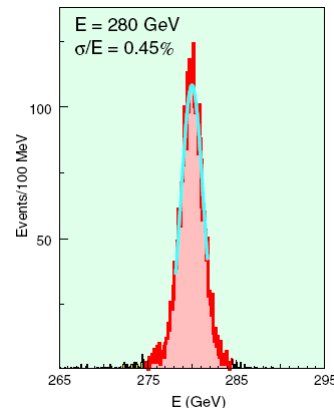
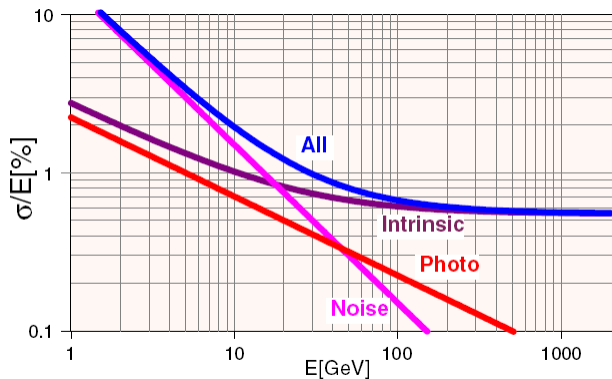


$$\frac{\sigma(E)^{\text{barrel}}}{E} = \frac{2.7\%}{\sqrt{E}} \oplus 0.55\%$$

$$\frac{\sigma(E)^{\text{endcap}}}{E} = \frac{5.7\%}{\sqrt{E}} \oplus 0.55\%$$

□ Endcap: preshower detector

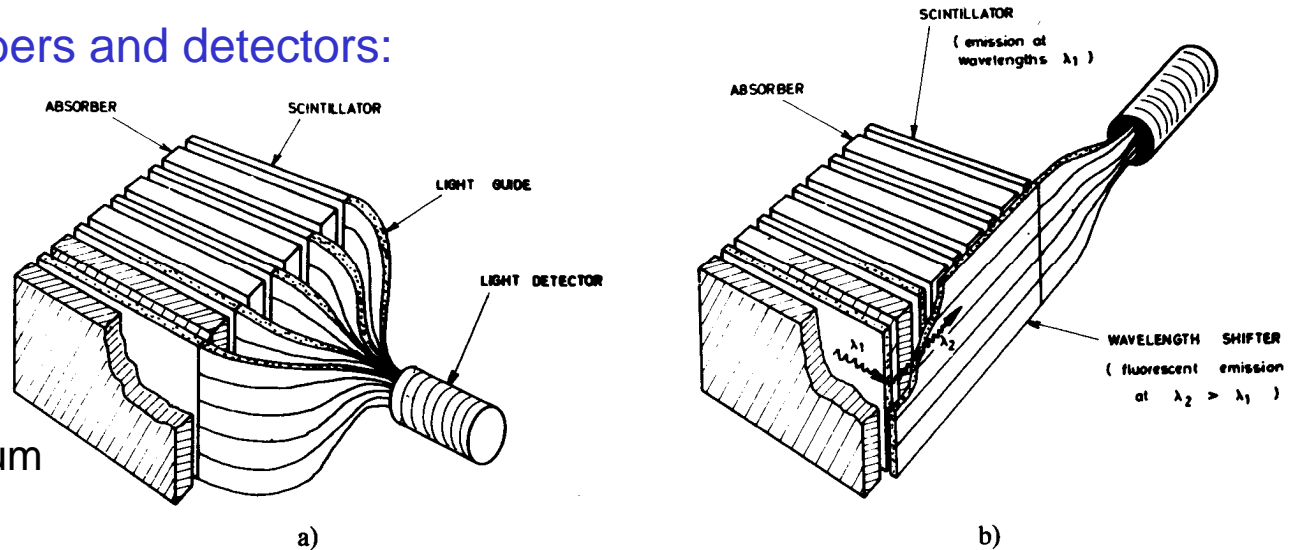
- 2 lead layers with Si-strip detectors at 1.9mm pitch
- impact resolution: $\sim 300\mu\text{m}$
- π^0 - γ separation:



- adds $5\%/\sqrt{E}$ to the stochastic energy resolution

Sampling Calorimeters

- Interleaved series of absorbers and detectors:

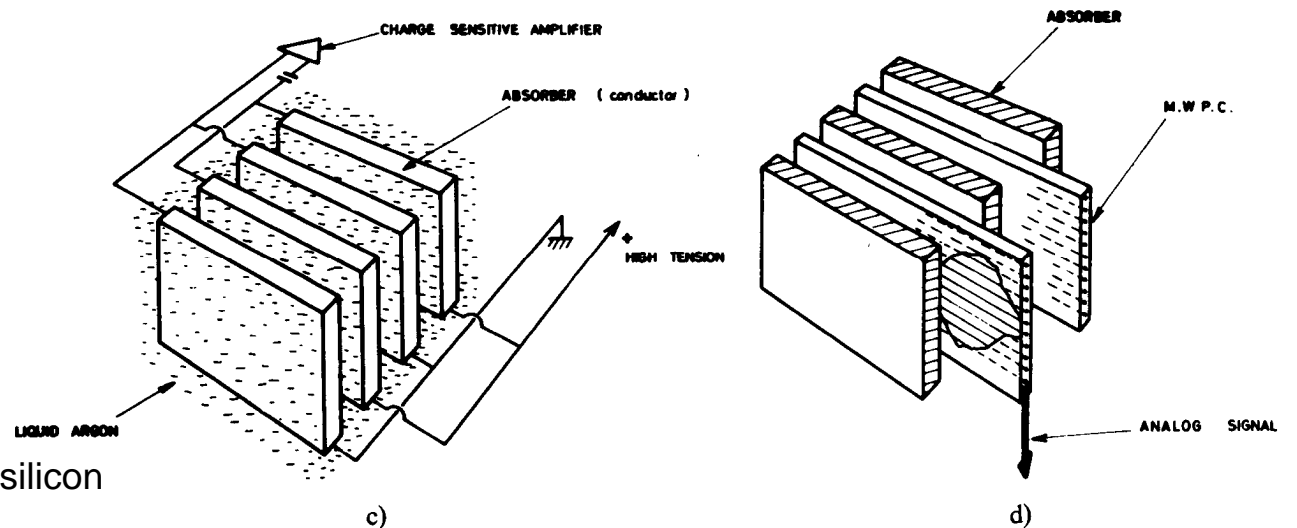


- Absorbers:

- iron, lead, tungsten, uranium

- Detectors:

- gaseous:
 - MWPCs, streamer tubes
- cryogenic liquid:
 - noble gases (Ar, Xe, Kr)
- warm organic liquid:
 - TMP, TMS
- solid:
 - scintillators, scint. fibres, silicon



Presampling Calorimeters

□ Sampling calorimeters:

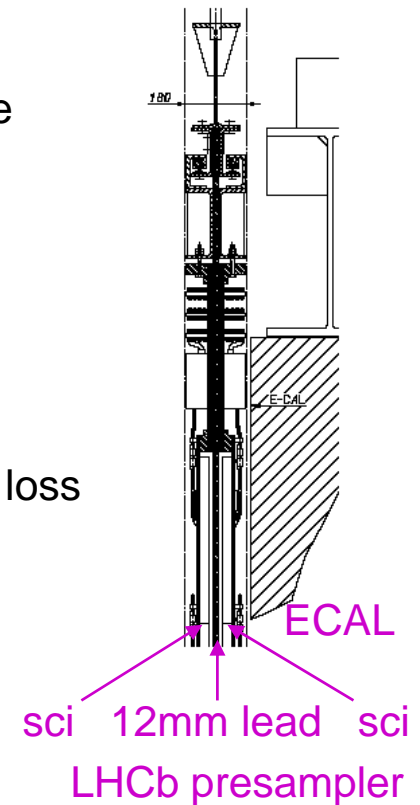
- channels with PMT readout and signal processing via ADCs are expensive
- several sampling volumes are combined into one readout channel
- cell volumes are large
- calorimeters are placed outside the tracking detectors

□ Dead material:

- e.g. beam pipe, detector enclosures, solenoids, support structures
- showering in these materials gives rise to secondary particles and energy loss

□ Presampling calorimeter:

- placed before el.mag. calorimeter
- one layer of scintillator with same or better cell resolution as calorimeter
- counts initial particle multiplicity entering the calorimeter
- gives estimate of showering and energy loss before calorimeter
 - correction possible → reducing error from fluctuation → increase energy resolution
- refinement1: a layer of absorber plus another layer of scintillator read out separately
 - absorber adds to dead material → second scintillator layer discriminates e and γ showers
- refinement2: Si-strip detector instead of scintillator → γ - π^0 separation from position resolution



Sampling Calorimeters I

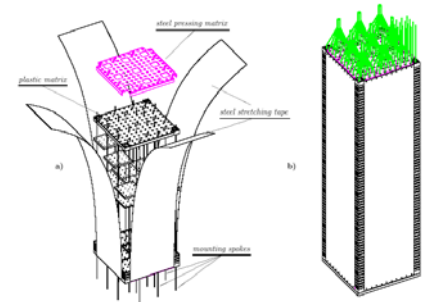
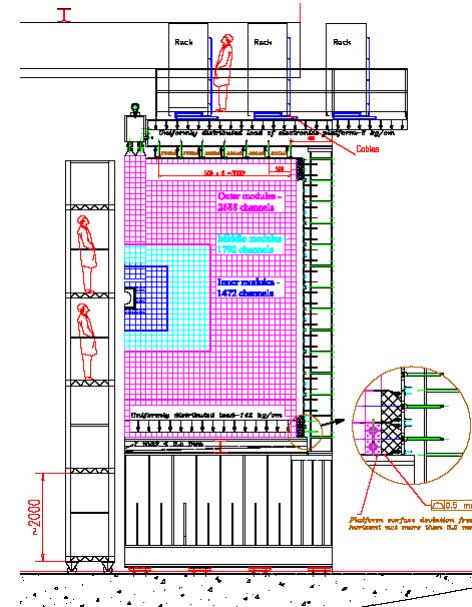
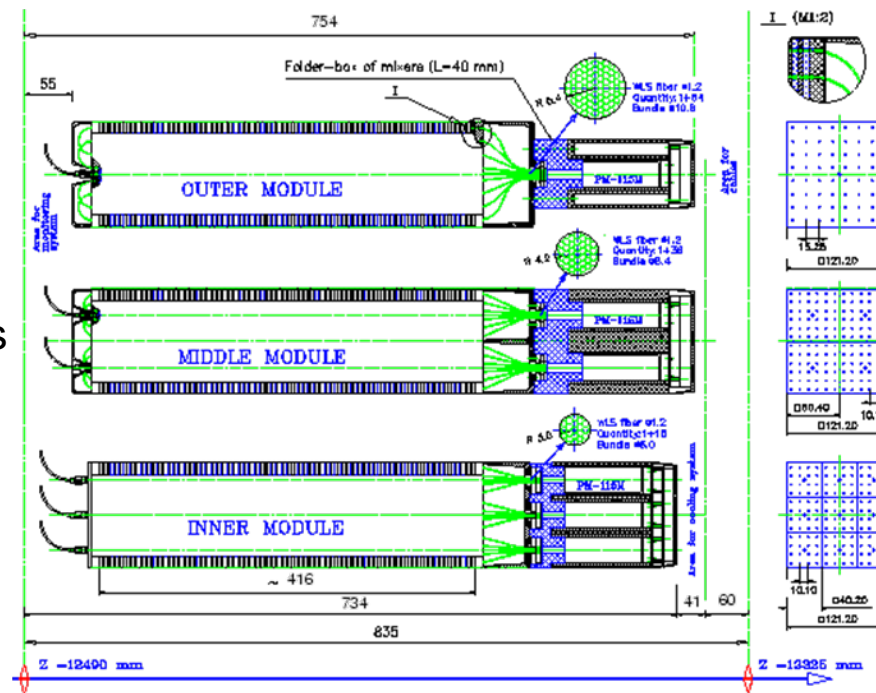
□ LHCb ECAL: “Shashlik” electromagnetic calorimeter:

- 66 layers of 2 mm Pb absorber plates
- interspersed with 4 mm scintillator tiles
- light collection with wavelength shifting fibres, turned round at front-end
- read-out by photo multiplier tubes
- thickness: $25 X_0$ or $1.1 \lambda_{had}$

- resolution:

$$\frac{\sigma(E)}{E} = \frac{10\%}{\sqrt{E}} \oplus 1.5\%$$

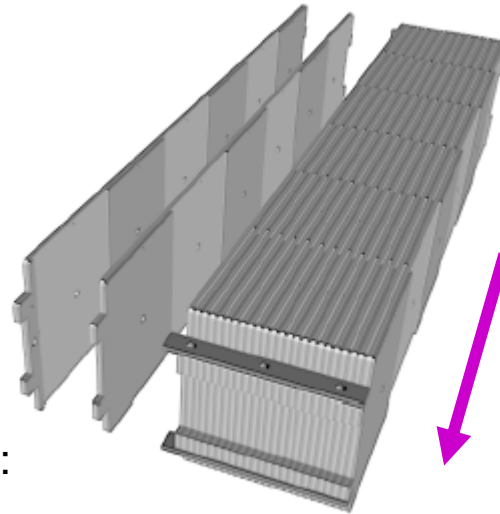
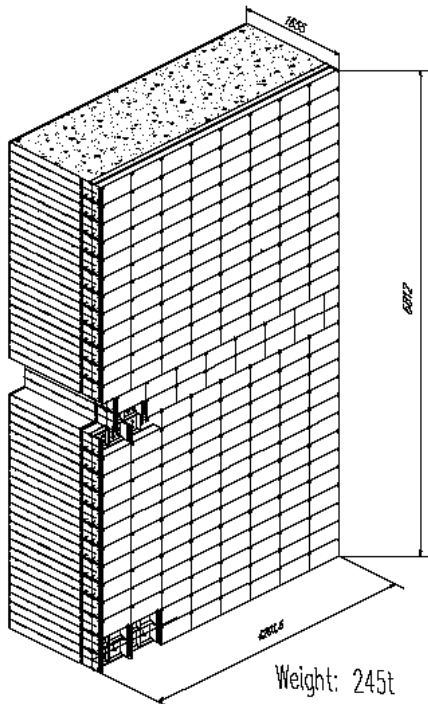
better only with crystals
→ too expensive



Sampling Calorimeters II

□ LHCb HCAL:

- 16 mm iron absorber plates, parallel to beam
- interspersed with 4 mm scintillator tiles, staggered
- light collection with wavelength shifting fibres
- read-out by photo multiplier tubes
- thickness: $5.6 \lambda_{\text{had}}$



resolution:

$$\frac{\sigma(E)}{E} = \frac{80\%}{\sqrt{E}} \oplus 10\%$$

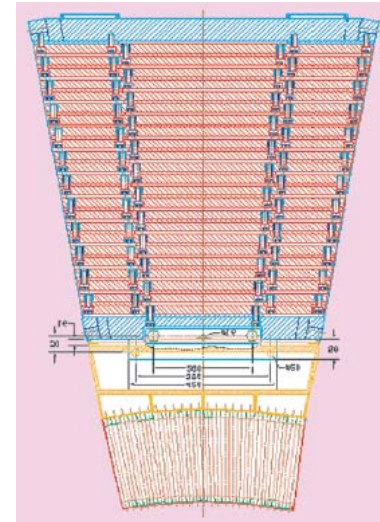
beam direction



Sampling Calorimeters III

□ CMS hadronic calorimeter:

- absorber 50mm copper (high density) + 4mm scintillator
- 1mm wavelength shifting and clear fibres
- cell size: $\Delta\eta \times \Delta\phi = 0.87 \times 0.87$
- pointing geometry, inside 4T solenoid
- not thick enough to contain high-E particles
→ further scintillator layers outside solenoid...
- full length (incl. solenoid): $\sim 11\lambda_{\text{had}}$
- resolution:

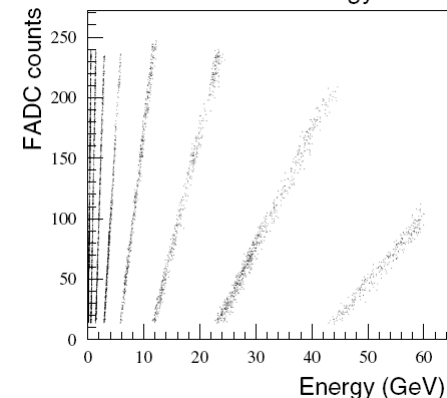
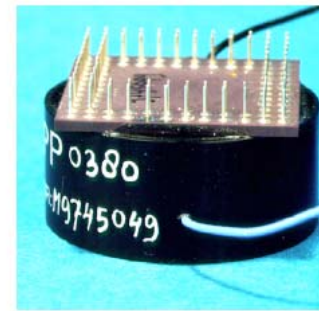
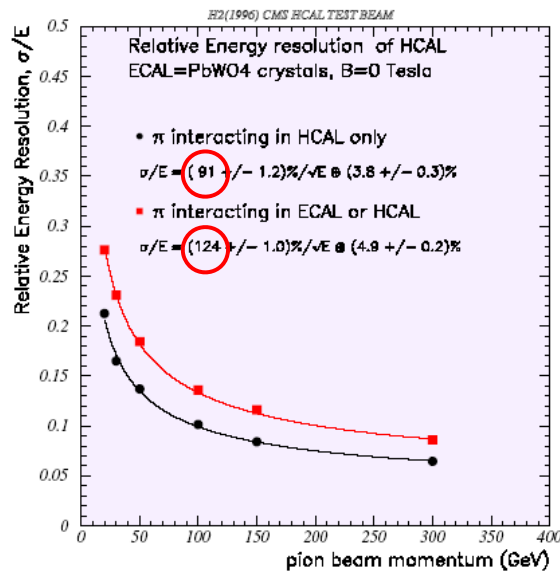


HCAL

ECAL

□ Readout:

- commercial 19- and 73-channel HPD at 10-15kV
- ok in high axial fields, linear up to 3TeV hadron showers
- huge dynamic range: multi-range FADCs



Sampling Calorimeters IV

□ ZEUS uranium calorimeter:

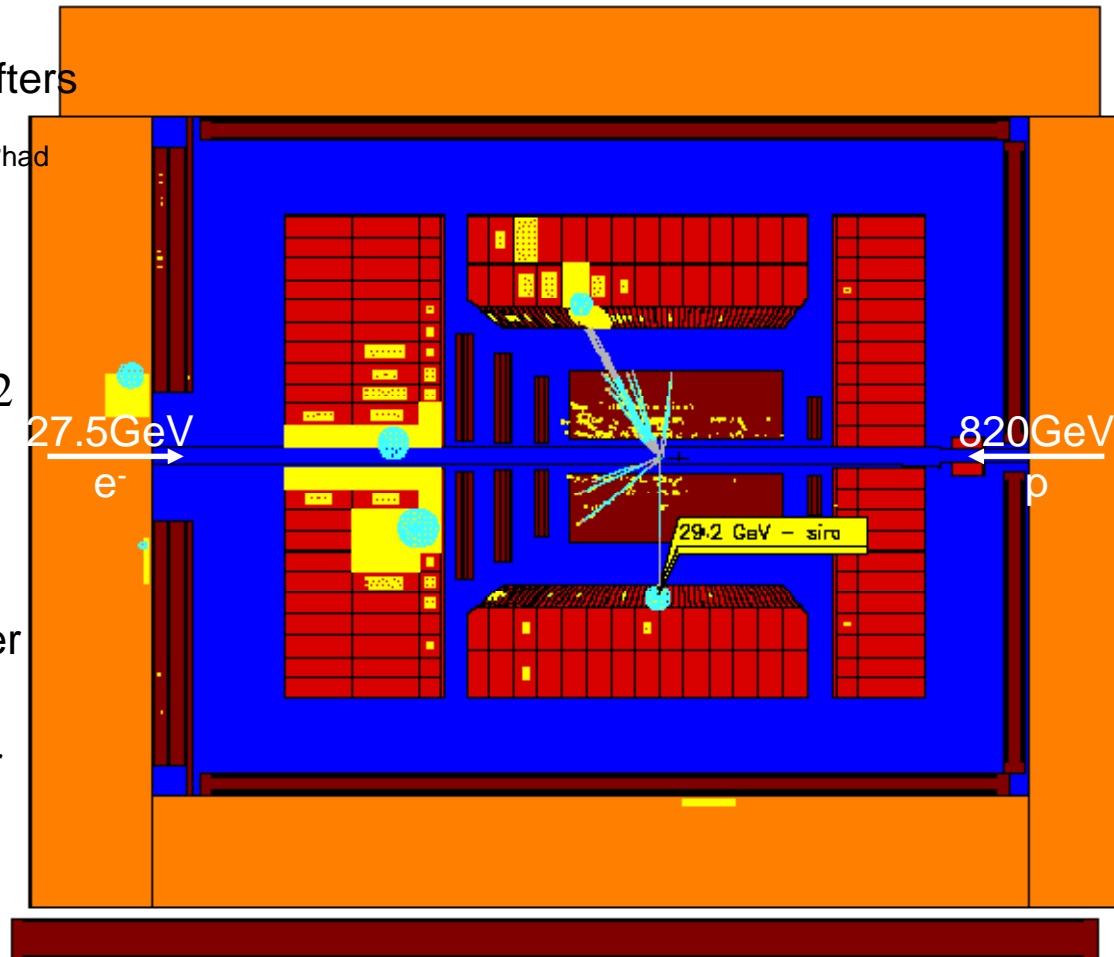
- 3000 tons of depleted U^{238}
- 11592 cells, $5 \times 20 \text{cm}^2$ - $20 \times 20 \text{cm}^2$
- double-sided readout via wavelength shifters
- thickness: EMC $22\text{-}30 X_0$, HAC $4.0\text{-}7.1 \lambda_{\text{had}}$
- time resolution: $\sigma_t \sim 1 \text{ns}$ ($>4.5 \text{GeV}$)

□ Compensation:

- special layout: el.mag. & had. showers have same energy yield: $\frac{e}{h} = 1.00 \pm 0.02$
- neutrons recoil off protons in scintillator
→ regenerate visible energy
- U^{238} gives additional n from spallation
→ smaller volume than for other absorber
- visible fraction e lower in high Z material
- adjust rel. thickness: absorber/scintillator
- resolution:

$$\frac{\sigma^{elmag}(E)}{E} = \frac{18\%}{\sqrt{E}} \oplus 1\% \quad \frac{\sigma^{had}(E)}{E} = \frac{35\%}{\sqrt{E}} \oplus 2\%$$

Particle Physics Detectors, 2010



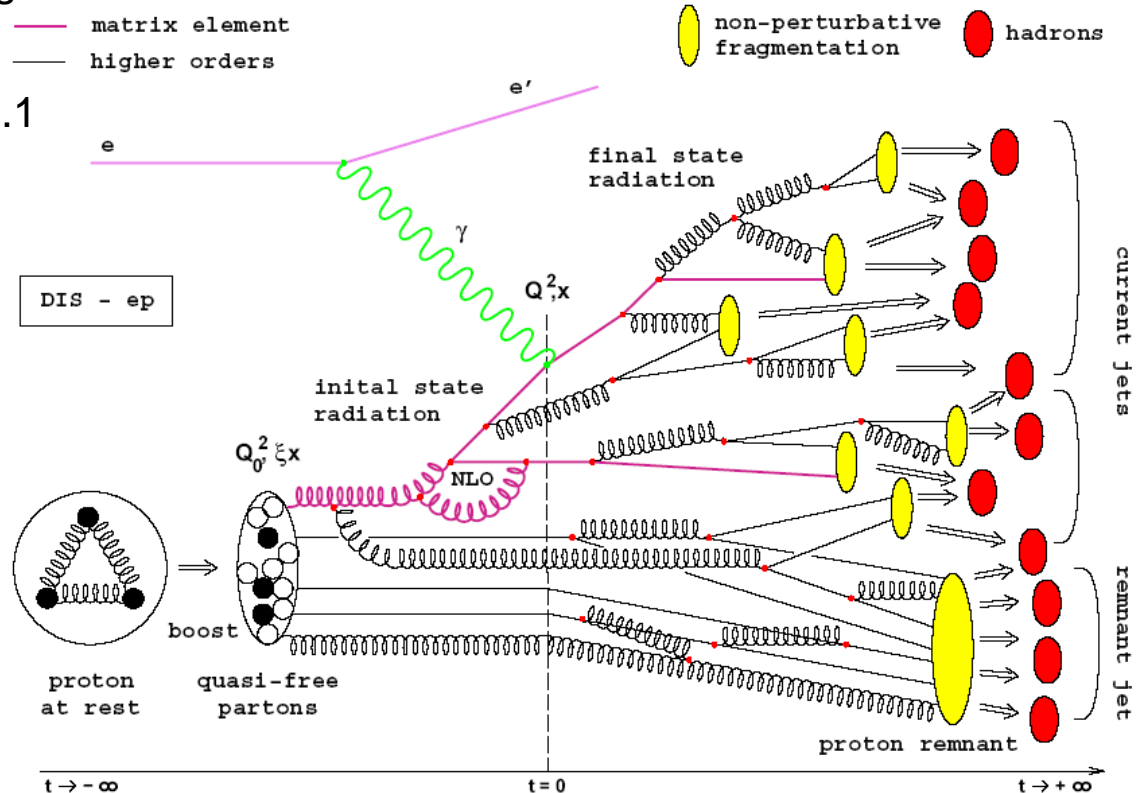
Stephan Eisenhardt

V/24

Event Kinematics

Example: deep inelastic ep-scattering

- combines features of e^+e^- and pp -scattering
- initial state: lepton + quasi-free partons
- el.mag probe: QED • $\alpha_{el} \sim 1/137$
- strong **hard** process: QCD • $\alpha_s \sim 1 \dots 0.1$
- **soft** (non-perturbative) fragmentation
- hadronisation → hadronic final state
- HFS features:
 - current jets (high p_T)
 - proton remnant (spectator jet)
- initial state radiation (el.mag.)
- final state radiation (el.mag. or strong)



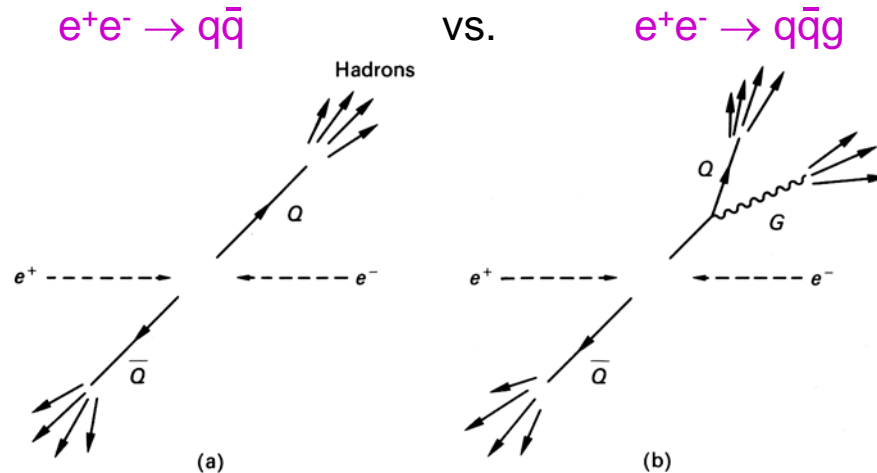
Kinematic variables:

- centre of mass energy: s
- Bjorken scaling variables:
 - $Q^2 = -q^2$: 4-momentum transfer
 - $x = Q^2 / 2pq$: momentum fraction of struck parton
- pseudo-rapidity: $\eta = -\ln \tan \theta/2$

Event Shapes

□ Global geometrical description of final state:

- predecessors of jet finding algorithms
- to distinguish classes of decay patterns
- e.g.



- theoretical predictions: usually on parton level (or NLO or NLL ...)
- without a good hadronisation model: no reliable comparison to hadronic final state
- but geometrical patterns of the hard processes can be predicted
- assuming that they are still visible after hadronisation → event shapes
- still of interest:
 - determine power ($1/Q^2$) corrections
 - α_s form their Q^2 dependence in e^+e^- and ep-scattering

Event Shapes - Examples

- Thrust:**

$$T = \max \frac{\sum_i |\vec{p}_i \cdot \vec{e}|}{\sum_i |\vec{p}_i|}$$
 - unit vector \vec{e} points to thrust axis
- Spherocity:**

$$S = \left(\frac{4}{\pi}\right)^2 \min \left(\frac{\sum_i |\vec{p}_i \times \vec{e}|}{\sum_i |\vec{p}_i|} \right)^2$$

- Jet broadening:**

$$B_C = \frac{\sum_i |\vec{p}_i \times \vec{e}|}{2 \cdot \sum_i |\vec{p}_i|}$$

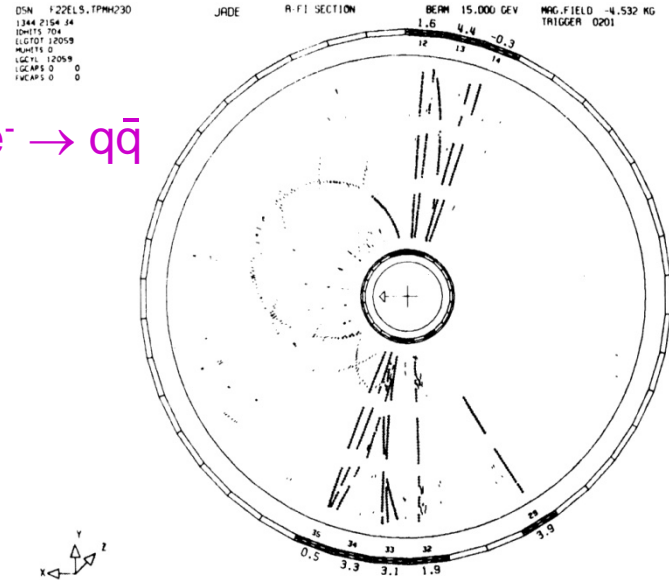
- Jet mass:**

$$\rho = \frac{M^2}{Q^2} = \frac{(\sum_i \vec{p}_i)^2}{Q^2}$$

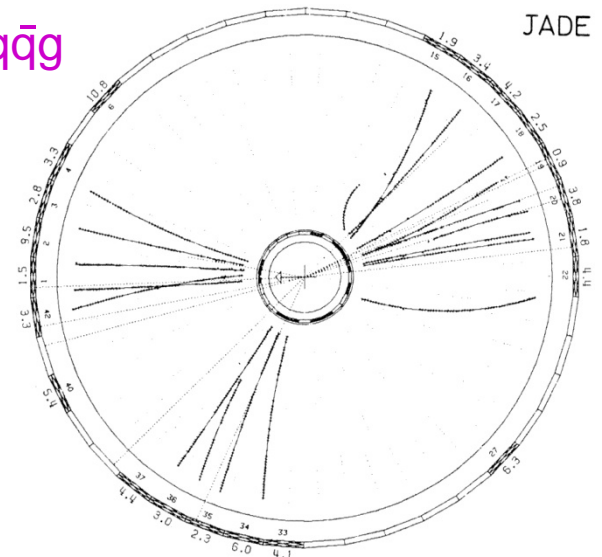
event shape	T	S	B_C	ρ
pencil like	1	0	0	1
spherical	1/2	1	1/2	0
$q\bar{q}g$	$\max\{x_i\}$	$\frac{16 \prod_i (1-x_i)}{\max\{x_i\}}$		

$$\text{with } x_i = \frac{2E_i}{\sqrt{s}}$$

$e^+e^- \rightarrow q\bar{q}$



$e^+e^- \rightarrow q\bar{q}g$



Particle Jets

□ What are jets?

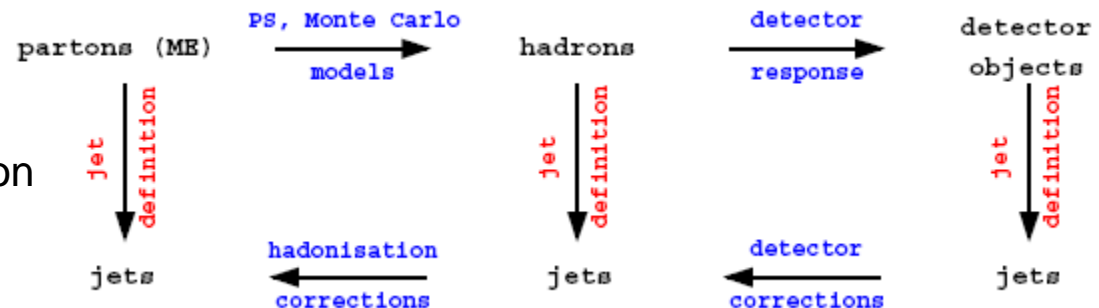
- quarks and gluons from hard scattering processes
- not observable directly
- but will appear as collimated flow of hadrons

□ Assumptions:

- jets carry the approximate 4-vector of the hard scattered partons
 - strong correlation for large Q^2
 - fails for low Q^2 at $\sim 1\text{GeV}$
- jet constituents are massless

□ Structure of jet analysis:

- prediction on parton level
- evolution via splitting functions: $q \rightarrow qq$, $g \rightarrow gg$, $g \rightarrow q\bar{q}$
 - exact ME calculation (NLO, NNLO)
 - parton shower model (LLA, NLL)
 - mostly soft and collinear
- further broadening due to hadronisation
 - but $p_{L,\text{jet}} \gg p_{T,\text{jet}}$



Jet Finding Algorithms

- Two classes:
 - geometrical algorithms: CONE(s)
 - simple concept
 - many slightly different implementations
 - practical problems with overlapping jets

 - cluster algorithms: JADE, K_T
 - more complicated definitions
 - but deterministic, i.e. no ambiguities
 - theoretical advantages

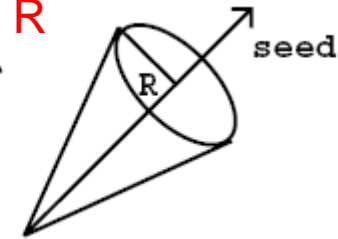
Jet Finding Algorithms I

□ CONE algorithm: maximise E_T flow through cone with radius R

- select cells (η, ϕ) with $E_{T,i} > E_{T,seed}$
- sum E_T in cone around seed
- if $E_{T,cone} > E_{T,min}$:
 - either stop
 - or iterate with new η', ϕ'

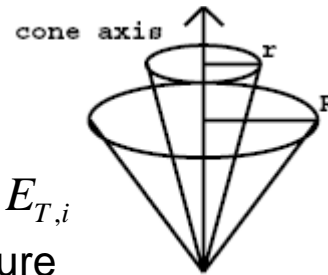
$$\Delta R = \sqrt{\Delta\eta^2 + \Delta\phi^2}$$

$$\eta = -\ln \tan \theta/2$$



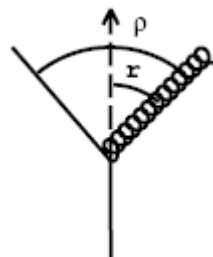
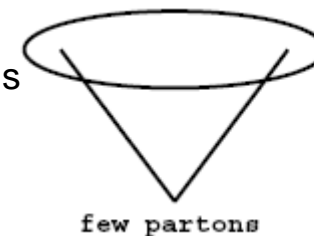
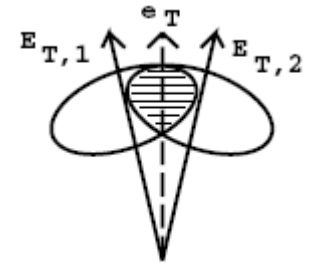
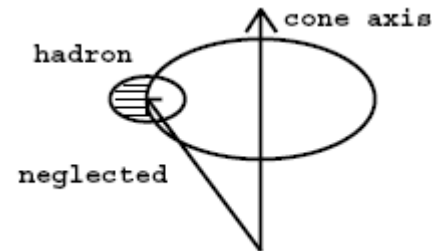
□ Advantages:

- easy energy correction $E_T^{jet} = \sum_i E_{T,i}$
- study internal (differential) jet structure



□ Problems:

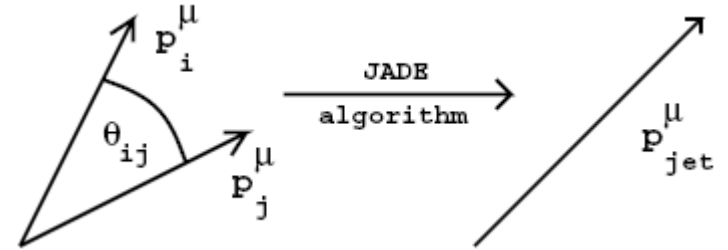
- sharp border cuts into 'underlying event'
- ad hoc choice to separate overlapping jets:
 - e.g. $e_T < 50\%$ of $E_{T,2} \rightarrow$ split into 2 jets
 - $e_T > 50\%$ of $E_{T,2} \rightarrow$ merge into 1 jet
- different behaviour for few and many particles:
 - artificial parameter R_{sep} needed in theoretical calculations to resolve hard radiation
 - one jet if: $r < R$ and $\rho < R_{sep}$
 - R_{sep} not universal



Jet Finding Algorithms II

□ JADE algorithm: cluster particles with minimal 'distance' in invariant mass

- for massless 4-vectors
- on detector level: introduce 'pseudo particle' for remnant
- calculate all distances: $m_{ij}^2 = 2E_i E_j (1 - \cos \Theta_{ij})$
- find minimum and recombine $\{i,j\}$ if: $\frac{m_{ij}^2}{M^2} < y_{cut}$
- energy scale: reference mass M^2 (usually = W^2 : total hadronic mass)
- resolution parameter: y_{cut}

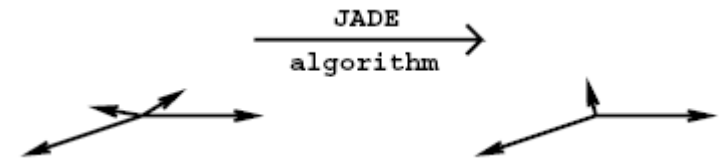


□ Advantages:

- covariant algorithm (defined in any reference system)
- allows factorisation of phase space (good for fixed order ME calculations)
- all particles will end up in a jet

□ Problems:

- remnant grabs much from the hadronic final state at lower η
 - large hadronisation corrections
- distance definition is 'non-local' in angle
 - production of 'phantom jets'
- how to recombine cells: Lorentz invariant, conserve E and/or \vec{p} , with or w/o scaling ...



Jet Finding Algorithms III

- k_T (Durham) algorithm: in BREIT frame: cluster particles with minimal distance in “transverse momentum” k_T

- Breit frame = brick wall frame for the probed particle

- clear separation between current and remnant region

- calculate all distances: $k_{T,ip}^2 = 2E_i^2(1 - \cos \Theta_{ip})$

$$k_{T,ij}^2 = 2 \min\{E_i^2, E_j^2\}(1 - \cos \Theta_{ij})$$

- find minimum and recombine $\{i,p\}$ or $\{i,j\}$ if:

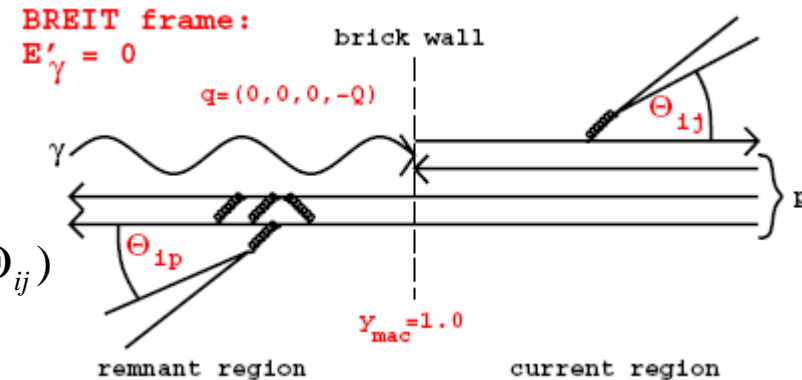
- **scale** = Q^2, p_T^2, k_T^2, \dots $\frac{k_{T,ij}^2}{scale} < y_{cut}$ or $\frac{k_{T,ij}^2}{scale} < y_{cut}$

- **Advantages:**

- can be used on parton/hadron/detector level in exactly the same way
- less sensitive to perturbation from soft particles
- supports analysis of internal jet structures by emission of secondary particles
- jet cross sections satisfy factorisation theorem → absolute predictions using PDFs possible
- k_T distance measure is suggested by coherence properties of soft QCD emission

- **Properties:**

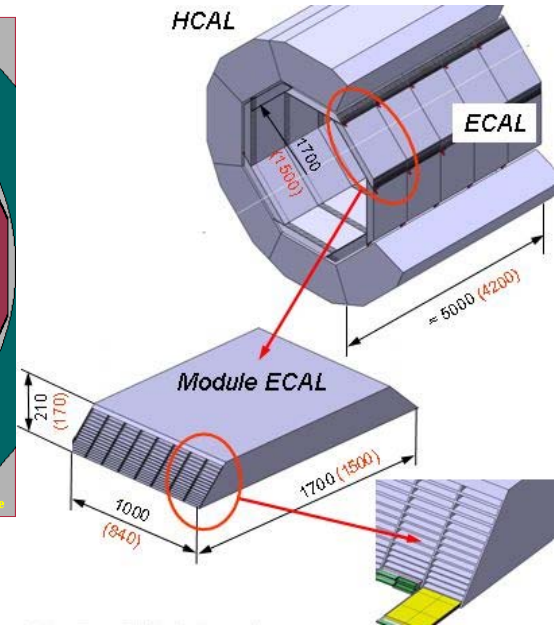
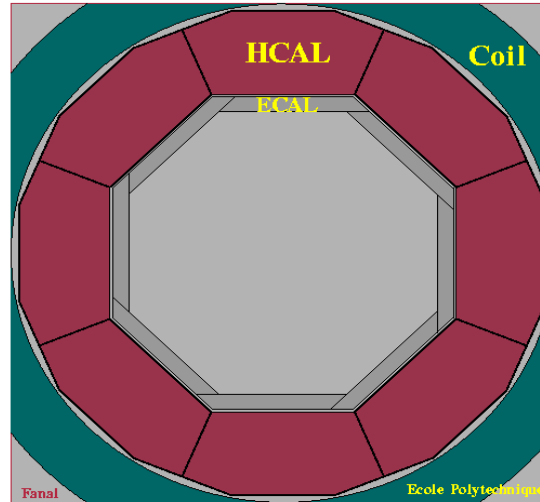
- remnant is spread over full detector
- “like” cone with event-by-event adjusted radius R



ILC CALORIMETRY

□ CALICE: Calorimetry for a Linear Collider Experiment: (option)

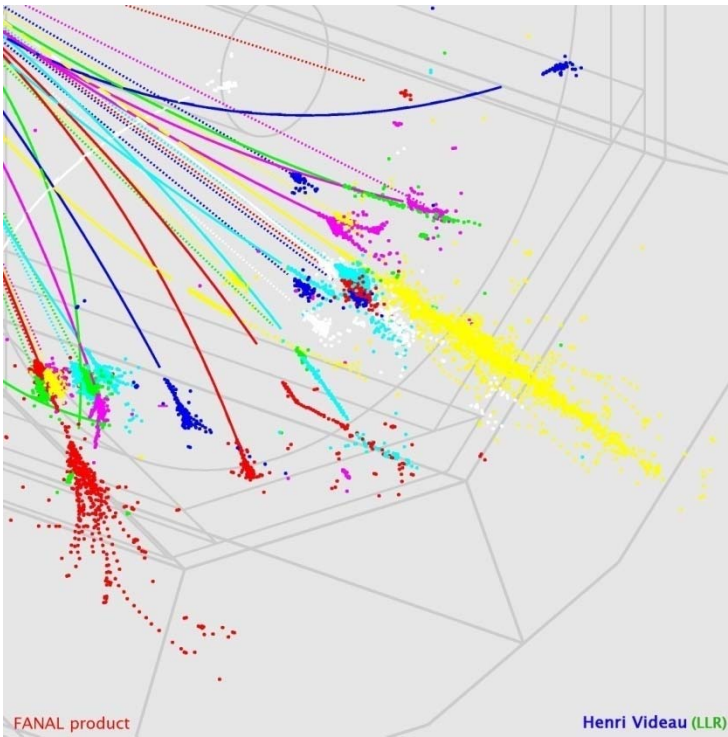
- ECAL & HCAL inside solenoid
- tungsten absorber:
 - small $X_0 \sim 3.5\text{mm}$
→ small thickness
 - small $R_M \sim 9\text{mm}$
→ defines size of el.mag. cell
 - comparably large $\lambda_a \sim 9.59\text{cm}$
→ hadron shower spreads wrt. elmag.



- Si-diode readout:
 - small diode pads: $\sim 1 \times 1 \text{cm}^2$
 - 3000m² of silicon, 38 million channels ($O(10^3)$ x today...)
- allows for the “tracking calorimeter”:
 - el.mag. shower is contained in 1+ 9 cells
 - had. shower: spreads, mostly one particle per cell...

Stephan Eisenhardt

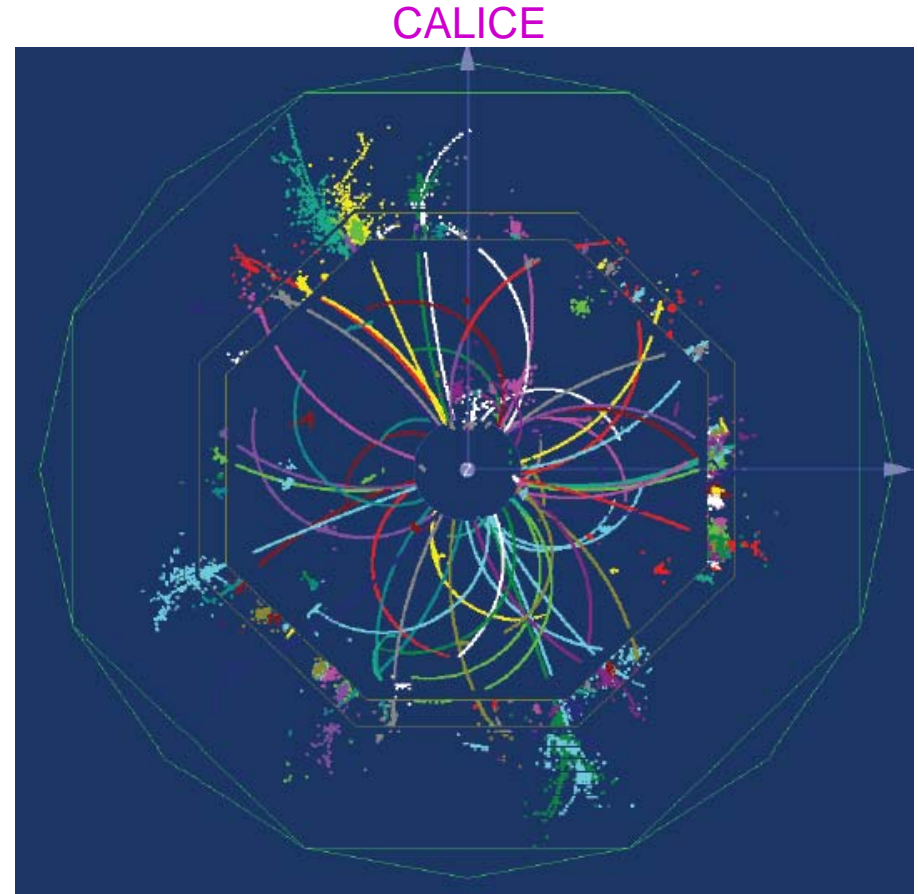
V/33



Particle Flow Algorithms

- Optimise jet energy resolution:
 - reconstruct each particle individually
 - use the best possible detector component
- Charged particles:
 - use tracking detectors
 - fraction of typical jet energy: ~65%
 - resolution: negligible
- Photons:
 - use el.mag. calorimeter
 - fraction of typical jet energy: ~25%
 - resolution: ~10%/√E
- Neutral hadrons:
 - use hadron calorimeter
 - fraction of typical jet energy: ~10%
 - resolution: ~40%/√E
- Average jet energy resolution:
 - naively: ~15%/√E
 - real world detector probably: ~30%/√E

Particle Physics Detectors, 2010



“tracking calorimetry”
gives additional detailed information
aim: reconstruction of neutrals

Stephan Eisenhardt

V/34